Chem Soc Rev

Supramolecular templating of hierarchically porous metal-organic frameworks

Journal:	*Chemical Society Reviews*
Manuscript ID:	CS-TRV-04-2014-000127
Article Type:	Tutorial Review
Date Submitted by the Author:	09-Apr-2014
Complete List of Authors:	Bradshaw, Darren; University of Southampton, Department of Chemistry El-Hankari, Samir; University of Southampton, Chemistry Lupica-Spagnolo, Lucia; University of Southampton, Chemistry

Journal Name

RSCPublishing

ARTICLE

Supramolecular templating of hierarchically porous metal-organic frameworks

Cite this: DOI: 10.1039/xoxxoooooox

Darren Bradshaw,*[a] Samir El-Hankari[a] and Lucia Lupica-Spagnolo[a]

Received ooth January 2012,
Accepted ooth January 2012

DOI: 10.1039/xoxxoooooox

www.rsc.org/

This tutorial review summarises recent advances in the direct supramolecular templating of metal-organic frameworks (MOFs) with hierarchical porosity across the micro- and mesoporous regimes. These are set against the important synthetic considerations that need to be addressed to ensure that strong interactions between the MOF precursors and a stable template assembly allow the highest chance of success. The article is grouped by template type and each category is illustrated with key examples and, where reported, an evaluation of their enhanced properties arising from the hierarchical structuring of the porous networks.

1. Introduction

1.1 Metal-organic frameworks

Metal-organic frameworks (MOFs) are crystalline inorganic-organic hybrid network structures assembled and sustained by coordination bonds between metal ions or metal-clusters and polydentate organic linking groups.[1,2] These highly ordered frameworks display permanent porosity, and through judicious choice of a large number of potential building blocks their structures, pore dimensions and functionality are readily tuneable.[3] MOFs are characterised by very high internal surface areas (typically $\geq$ 1000 m^2/g) and low crystal densities and are thus of significant interest for their potential in applications such as gas storage, molecular separation, catalysis, sensing and drug delivery.[4] As a result of the combination of metal ions and relatively small organic linkers, the vast majority of MOFs are classified as microporous, meaning their pore dimensions are < 2nm and adsorption behaviour is characterised by a type I isotherm. (Figure S1) As a result of this inherent microporosity, MOF applications tend to be restricted to small molecule separations and transformations where less efficient mass transport through these highly functional but relatively small coordination-based channels may provide an additional barrier to their widespread practical use. There are thus significant advantages to extending the porosity of MOFs into the mesoporous regime (fig S1), where pores in the range 2 – 50 nm are better able to meet the growing demands in the above applications, as well as challenges in energy storage and conversion, and the incorporation of large biomolecules.[5,6]

1.2 Mesoporous MOFs

Many MOFs do inherently exhibit mesoporous cages within their structures[7]; however, in the majority of cases these large cavities are accessed via much smaller apertures which limit the size of molecules that can diffuse into the functional void space. The preparation of mesoMOFs (mesoporous MOFs) through direct combination of metal ions and ligands by standard solvothermal synthesis methods is challenging[8], and there still remain few examples of truly mesoporous MOFs with ordered pores of dimensions > 2 nm running throughout the extended structure.[9] Synthetic strategies to increase the size of MOF pores are thus highly desirable, and largely involve the use of extended linkers and metal clusters to push pore metrics into the mesoporous regime. These methods have their advantages and disadvantages and references 7 and 8 provide a useful discussion of these. An alternative to increasing the framework micropore size is to employ a templating strategy where mesopores are formed within the microporous MOF.[10] (Scheme 1) This is particularly attractive, since the resulting materials will display hierarchical micro- and mesoporosity, combining the increased mass transport arising from the larger mesopores without loss of any of the high selectivity associated with much smaller micropores that is required for applications such as catalysis and separation.

1.3 Supramolecular templating

Since the discovery in the early 1990s that supramolecular or liquid-crystalline assemblies could be used to prepare mesoporous silicas[11], this has developed into the principal synthetic route for this class of materials[12] and has been successfully applied to a diverse range of inorganic and hybrid material compositions. This soft templating process is reliant on the ability of amphiphilic molecules such as surfactants (ionic and neutral) and block copolymers – termed structure-directing agents (SDAs) when used in this way – to readily self-assemble via non-covalent interactions into ordered mesoscale arrays.

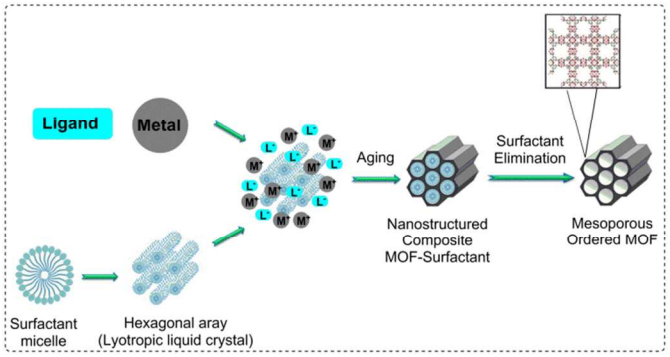

Scheme 1. Illustration of the idealized supramolecular templating of mesoporous MOFs arising from co-assembly of the SDA liquid crystal phase with the metal ions and ligands required for framework formation. (See also figure S2)

Templating of mesoporous oxide materials typically involves the co-assembly of the SDAs with appropriate inorganic precursors into a hybrid organic-inorganic mesophase.[13] Subsequent polymerisation or cross-linking of the precursors at the interface causes phase separation to occur, which effectively forms a continuous ordered oxide replica of the supramolecular organic mesoscale template. The final step is the removal of the SDA from the material, which involves calcination for the mesoporous oxides and other ceramics prepared in this way. Scheme 1 illustrates how the soft templating process can be applied to the preparation of mesoMOFs, where the inorganic precursors are replaced by the metal ions and organic linkers required for framework formation which co-assemble with the SDA. Cross-linking via metal-ligand bonding then occurs to form an extended functional microporous coordination network punctuated by an ordered array of mesopores.[10] Although many aggregates of MOF nanoparticles display textural mesoporosity arising from interstices between small particles, this tutorial review will focus only on those examples where a supramolecular template or SDA is reported to guide mesopore assembly. Figure S2 provides a brief discussion on the origins of hierarchical porosity in MOFs and highlights the differences between the various cases.

2. Important considerations for the templating of mesoMOFs

2.1 Interactions with the template

In order for the effective co-assembly of the metal ion and ligand building blocks for MOF formation with the SDAs, suitably attractive interactions between them are vital These interactions are well documented for the preparation of templated mesoporous silica[13], and are typically based on electrostatic or hydrogen-bonding between the precursors and the amphiphiles which are strongly dependent on reaction conditions, especially pH. In figure 1 we have attempted to rationalise a set of analogous interactions that could potentially occur between MOF precursors and the various types of charged and neutral SDAs available, classifying these using similar notation to that employed for silicas.[13] In section 3 it is clear that some of these interactions have already been observed; however, for templated mesoMOFs it is often difficult to assign these given the increased complexity of the self-assembly process over that observed for simple oxide structures.

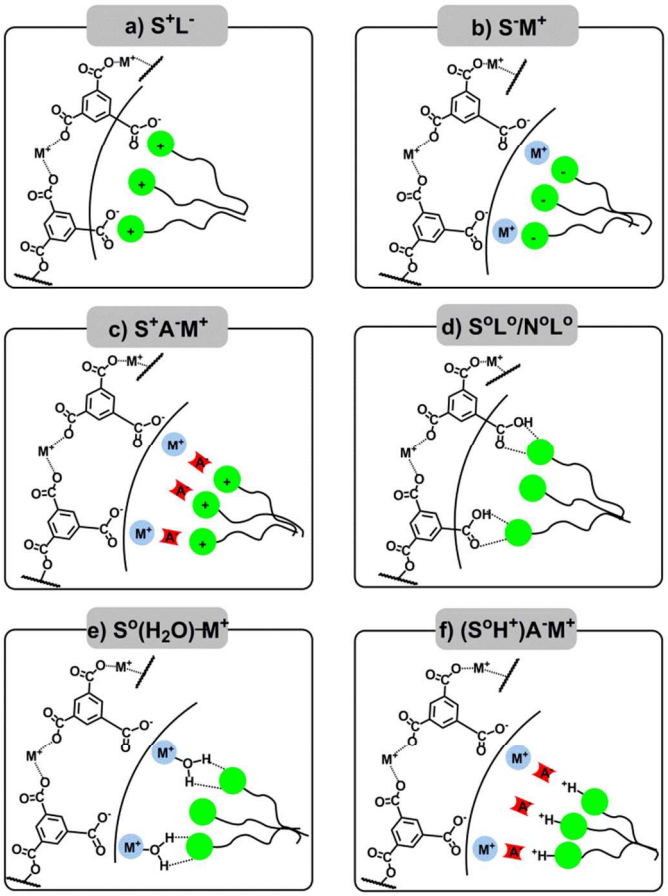

Figure 1. Potential interactions between charged and neutral SDA molecules and MOF precursors as illustrated for a typical carboxylate-based framework: S^+, S^- and S^0 are cationic, anionic and neutral surfactants respectively; N^0 is a block co-polymer template; A^- are anionic species; L^- the framework-forming ligands and M^+ the metal ions.

In the simplest case a direct electrostatic interaction can occur between a charged surfactant and a MOF building block of opposite charge. These interactions are written as $S^+L^-(M^+)$ and $S^-M^+(L^-)$ (figure 1a, b) using mesoporous silica-style notation, where S^+ and S^- are surfactants bearing cationic and anionic headgroups respectively, and L^- and M^+ the organic linkers and metal ions for MOF formation. Both mechanisms have previously been observed in mesoMOF templating[14, 15] as discussed in section 3.1. Templating strategies which include an intermediate species such as $S^+A^-M^+$ (fig. 1c) are also possible, where A^- is a counter-anion from the metal salt (or surfactant) or a deliberately added multi-anionic mediator species that can interact strongly with both metal ion and template.[16] Attractive interactions between the template and MOF precursors could also be mediated by hydrogen-bonding, where neutral surfactants (S^0) such as long-chain amines, or block copolymers (N^0), are employed as SDAs (fig. 1d,e). Such interactions could include direct hydrogen-bonding to the ligand, S^0L^0 (fig. 1d) or a metal-bound water or solvent molecule $S^0(H_2O\text{-}M^+)$ (fig. 1e). With some block copolymers it is necessary to protonate the template to induce self-assembly and mesophase formation: under these conditions a mechanism such as $(S^0H^+)A^-M^+$ (fig. 1f) become possible where the anionic species A^- could also be a deprotonated framework-forming organic linker (L^-).[17] It may also be possible to achieve a direct coordination bond between a surfactant headgroup (*e.g.* an anionic group or a neutral

amine) and the metal ion for MOF formation, which could be facilitated by use of metal ions with appropriate hardness.

2.2 Synthetic conditions

Just like for the formation of mesoporous silica[12, 13], pH is an extremely important parameter for the successful templating of mesoMOFs as it plays a defining role in the type and strength of interactions between the precursors and template, affects rates of metal-ligand complexation through modulation of ligand protonation/deprotonation equilibria and for some block co-polymers is critical to the self-assembly process. If we consider a simple electrostatic S^+L^- mechanism (fig 1a), it is clear that the interactions between them will be most attractive when the surfactant and organic linker are in appropriate protonation states *e.g.* a positively charged amine surfactant ($pK_a \sim 9$) and a carboxylate-based linking group ($pK_a \sim 3$-4) at approximately neutral pH. This is readily controlled at the synthesis stage, unless a drastic pH change occurs during co-assembly and/or framework formation.

For MOF synthesis there is a strong driving force for metal ions to rapidly complex suitable ligand species to form thermodynamically stable extended lattice structures. If this happens too readily however, phase separation will occur before co-assembly of the precursors and the SDA which will prevent effective templating. MOF chemists have developed several strategies to control the rates of framework nucleation and crystal growth[18] however, which is usually affected by modulating the chemical potential of the metal ions or ligand deprotonation rate using suitable additive molecules. For example, a monodentate non-framework propagating ligand is often added to complex the metal ion thus providing a competitive ligand to slow down framework formation. In the case of mesoMOFs, the addition of such a modulator has the potential to not only control coordination kinetics and interactions with the SDA to aid the templating process, but could also provide a degree of control over the resultant crystal size potentially leading to coordination-derived analogues of mesoporous silica nanoparticles (MSNs) that are widely employed for drug delivery applications.[19]

For the templating of mesoporous materials, it is the supramolecular template aggregates which control the mesopore size and the nature of the mesostructure, and are thus readily tuneable by SDA choice. However, this is only valid if the synthetic conditions necessary to prepare the desired material are compatible with those of template assembly. As outlined above pH is very important, but the nature of the solvent and reaction temperature will also play a key role as will the order of addition of the precursors. (Section S3) It is clear that controlling or balancing the above parameters in the context of the stability of the template aggregates, reaction kinetics and the expected interactions between the SDA and the metal ions and ligands will be critical to the success of the supramolecular templating of mesoMOF materials. This will undoubtedly be MOF specific, and conditions will need to be optimised for the diverse range of MOF families already reported.

2.3 Template removal

The final consideration is the removal of the SDA from the resulting mesoMOF in order to fully access the large templated pores within the structure. As outlined above, this is done via calcination of thermally stable oxide phases by heating to temperatures around 500 °C. Most MOFs are not stable to temperatures in this range so the template molecules will need to be eliminated by some other method. This commonly involves exhaustive solvent extraction in order to fully remove the template, and for this reason neutral rather than ionic SDAs are likely to be favoured. It should also be noted that in some cases, removal of the template from mesoporous coordination-based solids causes the mesopores to collapse so stabilising these is also a challenge.

3. Templated mesoporous MOFs

3.1 Templating with cationic structure-directing agents

By far the most work reported on the templating of mesoMOFs using ionic surfactants as SDAs has involved cationic amphiphiles. Hierarchically micro- and mesoporous HKUST-1 ($Cu_3(BTC)_2(H_2O)_3$ where BTC = 1,3,5-benzenetricarboxylate) as reported by Qiu et al[14] was the very first example of a supramolecularly templated mesoMOF. This involved the synthesis of the industrially relevant HKUST-1[20] in the presence of the widely used cationic surfactant CTAB (cetyltrimethyl ammonium bromide, fig S4), which was simply added to the standard solvothermal synthesis of the MOF in a water/EtOH solvent mixture. The CTAB micelles were found to template hierarchically porous HKUST-1 phases with adjustable porosity, where the specific mesopore surface areas and volumes increased with the CTAB/Cu^{2+} molar ratio such that more mesoporosity is observed with higher amounts of the SDA. After removal of the SDA by solvent extraction, all materials displayed a N_2 adsorption profile intermediate between type I and type IV (figure 2a), arising from the micropores of the MOF and the templated mesopores respectively, and also exhibited pronounced hysteresis loops on desorption. An analysis of the pore size distributions (figure 2b) for the sample prepared from a CTAB/Cu^{2+} ratio of 0.6 revealed micropores with a diameter of 0.8 nm and mesopores of 5.6 nm, consistent with a 3-D network of interconnecting pores where the mesopore walls in these solids are formed from a crystalline microporous framework.

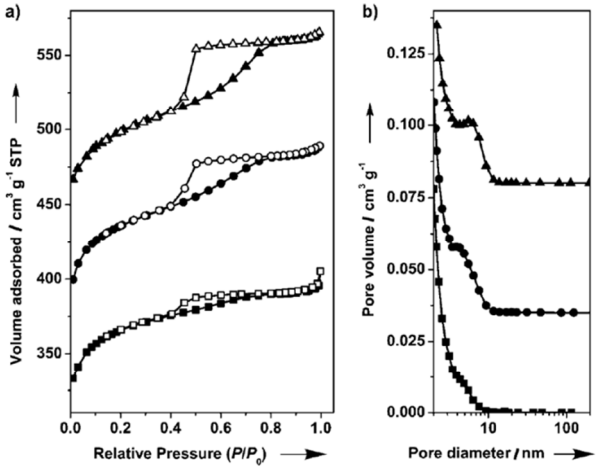

Figure 2. Pore-structure analysis of hierarchically micro- and mesoporous HKUST-1 prepared at various mole ratios of Cu^{2+}/CTAB: 1:0.15 (squares), 1:0.3 (circles) and 1:0.6 (triangles). a) N_2 adsorption–desorption isotherms; the isotherms for 1:0.3 and 1:0.6 are vertically offset by 100 and 200 cm^3 g^{-1}, respectively. b) Distributions of pore diameters obtained using the Barrett–Joyner–Halenda (BJH) method; the distributions for 1:0.3 and 1:0.6 are vertically offset by 0.035 and 0.08 cm^3 g^{-1}, respectively. (Reprinted with permission from ref. 14. Copyright 2008 Wiley-VCH)

Using supramolecular templating strategies, the mesopore diameter is strongly dependent on the hydrophobic volume of the self-assembled amphiphiles where an increase in surfactant chain length or hydrophobic component in block copolymers will lead to larger pores. A common method to increase mesopore size is thus to swell the micelles using an auxiliary SDA such as 1,3,5-trimethylbenzene (TMB); this is incorporated into the hydrophobic interior thus expanding the micelle. By adding TMB to the CTAB templated HKUST-1 synthesis the mesopore size can readily be increased from 5.6 to 31.0 nm using a CTAB/TMB ratio of 0.5.

Diffraction and electron microscopy data (figure 3) show that a disordered wormlike mesostructure without long-range order is obtained for the mesoMOF which is composed of nanocrystalline domains, and while templating via an S^+L^- mechanism seems most likely in this case, the exact nature of the mesophase formed by assembly of the SDA under the solvothermal synthesis conditions required for the framework is not currently clear.

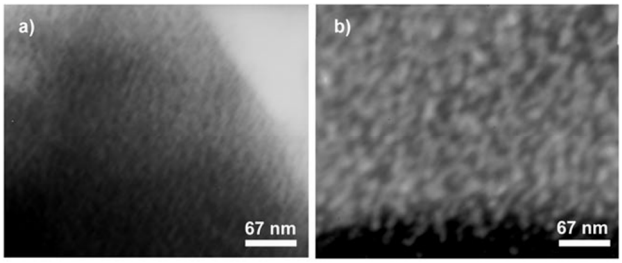

Figure 3. TEM images of mesostructured HKUST-1 prepared in the presence of CTAB with (a) and without (b) TMB as a swelling agent. (Reprinted with permission from ref. 14. Copyright 2008 Wiley-VCH)

The same group used an identical CTAB/TMB templating strategy to prepare hierarchically porous MIL-101, which resulted in a meso-/macroporous system[21]: the mesopores arising from the large-pore MIL-101 and the macropores from the interparticle space between the large aggregated nanocrystals. While the hierarchically porous MOF displays significantly enhanced dye adsorption kinetics over the standard MIL-101, it is clear from microscopy images that this is not a templated material as defined in figure S1b. This confirms that synthetic conditions are very important to successful templating, and the acidic MIL-101 synthesis media potentially disrupts the S^+L^- mechanism leading to nanocrystal rather than mesopore formation as in the case of meso-HKUST-1.[14]

Mesoporous HKUST-1 using CTAB as the SDA has also been prepared in the presence of citric acid (CA) as a co-template.[16] The CA was employed to rationally adjust the interactions between the cationic template and the precursors, where this multi-anionic species could increase such interactions via both electrostatics and chelation of the metal ions. (Figure 4) It was found that mesoMOFs only formed in the presence of the cooperative template, but not when CTAB or CA was used alone in the solvothermal reaction carried out in DMF. This is in contrast to the work of Qiu et al[14] who successfully prepared meso-HKUST-1 templated only by CTAB in $EtOH/H_2O$, which clearly illustrates the importance of solvent in the assembly process. In the presence of the cooperative CTAB/CA template however, hierarchically micro- and mesoporous HKUST-1 is prepared with a maximum mesopore diameter of 19.6 nm at the optimum CTAB/CA molar ratio of 2.3:1 below this few mesopores are formed due to reduced interactions between the templates, while at high quantities of CA a competing phase is identified by diffraction measurements. The structure-directing effect is attributed to an $S^+A^-M^+$ (fig. 1c) type mechanism, where CA (A^-) interacts simultaneously with the metal ions and surfactants establishing a well-defined chemical interaction between the micelles and precursors to effectively direct nucleation and crystal growth within the continuous solvent region. Again, microscopy reveals the mesopore structure to be disordered.

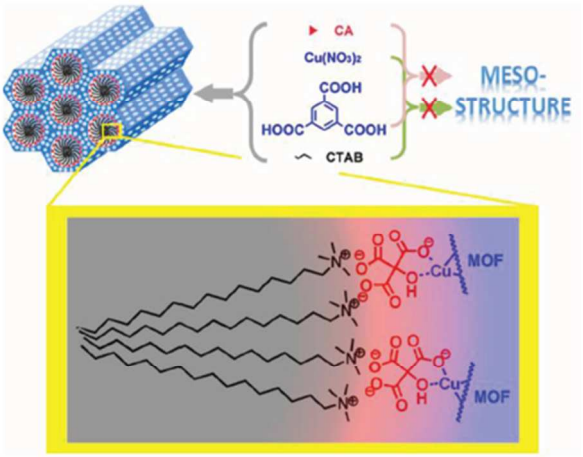

Figure 4. Schematic representation of the cooperative template-directed synthesis of mesoporous HKUST-1 using CTAB and citric acid as SDAs. (Reprinted with permission from ref. 16. Copyright 2012 American Chemical Society)

In the same synthetic system, Wee et al. also report a double-templating approach for the construction of a bimodal micro-/mesoporous hexagonal variant of HKUST-1 (known as COK-15) with permanent wide mesopores of 5 nm separated by microporous walls.[22] This method involves a Keggin-type phosphotungstate (HPW) anion alongside the cationic CTAB as SDAs. The Keggin ions serve as molecular templates for the structural motif of the MOF since they fit exactly into one of the cage-like pores, while CTAB directs these units into an ordered mesoporous structure as previously observed. The HPW anion in this material is occluded in the cavities constituting the walls between the mesopores (fig 5, top) and serves to enhance the stability of the resulting mesoMOF, permitting detailed diffraction and electron microscopy studies. As shown in figure 5 (bottom), TEM images clearly reveal a highly ordered mesopore structure with long-range order and a repeat distance (pore width) of 3.6 nm. The structure-directing role of CTAB in the formation of COK-15 is thought to be two-fold: CTAB inclusion in the pores during synthesis changes the pore topology to mesoporous, while CTAB in solution and external to the pores directs crystal morphology toward the observed extended flat slabs.

Hierarchically porous COK-15 was found to be highly catalytically active for the alcoholysis of styrene oxide under mild conditions.[22] In the presence of methanol at 40 °C, heterogeneous catalysis with COK-15 achieved 100% conversion of styrene oxide with 100% selectivity for 2-methoxy-2-phenylethanol after 3 hr of reaction. The reference compounds HKUST-1 and a microporous analogue with an encapsulated Keggin ion, HPW@HKUST-1, only reached 2 and 40% conversion respectively, indicating that the acidic HPW ion is responsible for the catalysis and the templated

mesoporosity of COK-15 permits highly efficient mass transport of the substrates and products.

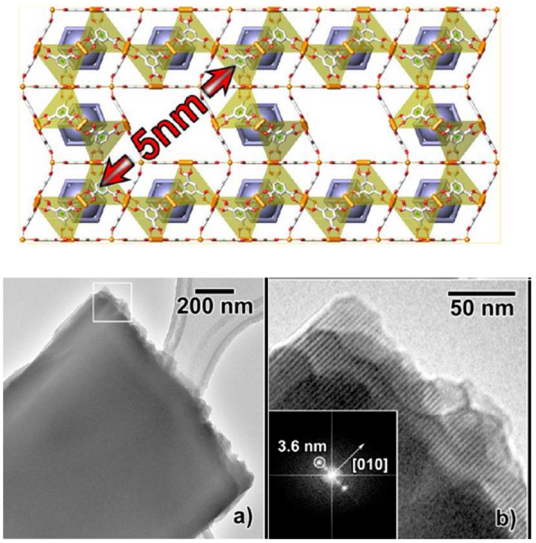

Figure 5. (Top) Structural representation of hierarchically porous COK-15, showing the position of the keggin anions (blue polyhedra) within the framework cages, and the location of the mesopores. (Bottom) TEM images of COK-15 showing (a) a typical bright-field image of the flat slab-like crystals. (b) an enlarged image of the region indicated in (a) showing the pore repetition. Inset: Fourier transform demonstrating a pore spacing of 3.6 nm. (Adapted with permission from ref. 22. Copyright 2012 American Chemical Society)

As noted in section 2.2, the formation of mesoMOFs via cooperative self-assembly between SDAs and MOF precursors is strongly dependent on the kinetics of coordination since the metal ions and bridging ligands have a strong tendency to crystallise, leading to macroscopic phase separation and template exclusion. This has been demonstrated by Huo and co-workers, who reported that mesoMOFs could not be prepared from Cu^{2+} when combined with H_3BTC or H_2BDC (BDC = 1,3-benzenedicarboxylic acid) ligands under hydrothermal conditions in the presence of a CTAC (cetyltrimethyl ammonium chloride) SDA.[23] They rationalised this was due to the strong coordination force between the metal ion and the carboxylate-based linking groups when compared to the hydrophilic head group of the surfactant. To overcome this, they devised a strategy to form mesoMOFs from 5-OH-BDC (5-hydroxy isophthalic acid), a linking group that contains weakly bonding hydroxyl groups and more strongly coordinating carboxylates. Here the hydroxyl functionality should interact with the SDAs to overcome the lattice stability and enhance cooperative self-assembly, whereas the carboxylate is present for framework formation. This combination of two functionalities with differing metal-binding capabilities into one ligand has indeed successfully led to a series of ordered mesoMOFs with 2-D hexagonal symmetry, where increasing the CTAC chain length from C_{14} – C_{18} leads to a corresponding increase in unit cell size. For the mesoMOF Cu-(5-OH-BDC)-C_{16} the mesopore repeat length is ~ 4 nm. It is noted that in this case the mesoMOFs (or rather the mesopore walls) are amorphous rather than crystalline, although spectroscopic studies point toward a chain-like construction where mononuclear Cu^{2+} ions are bridged by the 5-OH-BDC ligands.

The same authors also investigated the formation of mesoMOFs in the presence of a range of quaternary ammonium surfactants with varying charge densities and headgroup structures to examine their effect on mesostructure and crystal morphology.[24] It is known that the interfacial charge density between inorganic precursors and surfactant head groups plays a role in determining the final phase for mesoporous oxides[13], and while formation of mesoMOFs is more complex such charge-matching is also likely to be important. By modulating charge density of the surfactant, cubic mesophases with disordered Pm-3n symmetry, 2D hexagonal and lamellar mesophases of powdered Cu-(5-OH-BDC) were successfully prepared under low surfactant concentrations. In contrast to the hexagonal mesophases of Cu-(5-OH-BDC) templated by CTAC (or CTAB), the dicationic surfactant C18-3-1 (fig S4) directs assembly of a cubic Pm-3n mesophase of this framework. The headgroup of C18-3-1 bears two quaternary ammonium groups and its large size leads to the generation of high-curvature micelles favouring the formation of cage-like mesostructures, and it is proposed that the charge-matching between these micelles and the MOF is the key factor in preparing the observed cubic mesoMOF. Comparing their synthesis results with that for mesoporous silica SBA-1 of Pm-3n mesostructure prepared under acidic conditions**,** the authors rationalise that the assembly of cubic Cu-(5-OH-BDC) proceeds via the analogous $S^+A^-M^+$ (fig. 1c) formation pathway.

When the quaternary ammonium surfactants are employed in high concentration, they not only play a template role but also affect the size of the product. For example, discrete size-controlled mesoMOF spheres of Cu-(5-OH-BDC) were obtained in the size range 200 – 600 nm when increasing the CTAC concentration and adjusting the ratio of ligand:surfactant. This is consistent with previous studies where the addition of cationic surfactants to MOF syntheses provides a facile means to influence crystal size and morphology.[25]

Zeolitic imidazolate frameworks (ZIFs)[26] are 4-connected tetrahedrally coordinated networks of general formula $M(IM)_2$ where M = Zn(II) or Co(II) and IM = a 2-substituted imidazole linking group. ZIFs mirror the topologies observed for the aluminosilicate zeolites owing to the similarity between the M---IM---M bridging angle of 145° and that observed for the Si---O---Si links in, for example, silicate. They exhibit greater chemical and thermal stability than most other MOFs, and have applications in capture and storage of carbon dioxide and are often configured as supported membranes for the separation of hydrogen from gas mixtures.[27, 28] While a number of chemically diverse ZIFs with high surface areas have been reported, their pore apertures are typically very small (3 – 4 Å); hence as a class of material, ZIFs would significantly benefit from templating strategies to enhance their properties through improved mass transport.

The first mesostructured zinc imidazolate frameworks were prepared by Lotsch and co-workers[29] by reacting suitable imidazole ligands with zinc acetate under reverse microemulsion conditions in the presence of CTAB or its longer chain analogues. In this system, the quaternary ammonium species acts as a template giving rise to mesostructured imidazolate frameworks (known as MIFs) which are distinct from the extended network ZIFs prepared from the same ligands. The MIFs are lamellar hybrid structures composed of 1D zinc imidazolate chains terminated with Br^- anions that are electrostatically bound to the interdigitated CTAB cations which interleave the layers. (Figure 6) The basal spacing between the layers depends on the size of the anion which accompanies the cationic surfactant and the size of the imidazole ligand, and is further tuneable by the length of the

surfactant alkyl chain. The composite MIF phases display bimodal organisation rather than hierarchical porosity, which clearly demonstrates the importance of synthetic conditions to the formation of mesoMOFs. Interestingly, treating MIF-1 (2-methylimidazole ligand) in EtOH at 100 °C to effect removal of the CTAB quantitatively converts this to the corresponding microporous network structure ZIF-8.

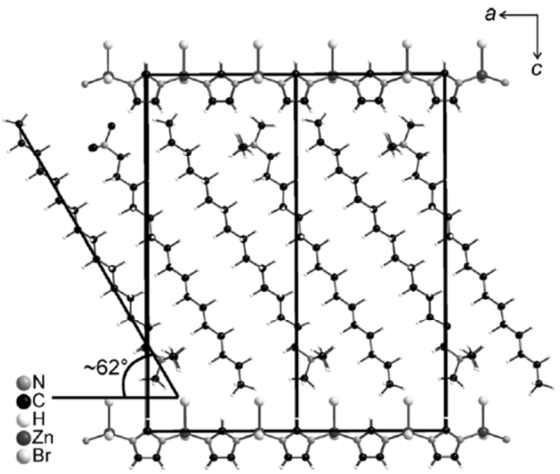

Figure 6. Structural model of a typical mesostructured imidazolate framework (MIF) showing the zinc-imidazolate layers with CTAB oriented between. (Reprinted with permission from ref. 29. Copyright 2012 Wiley-VCH)

Although hierarchically porous ZIFs were not accessible from this reverse microemulsion-based reaction system, such surfactant mediated synthesis and subsequent exfoliation of the lamellar composites can be successfully employed as a strategy for the direct preparation of ultrathin coordination polymer nanosheets.[30] When benzimidazole (BeIM) is employed as the framework linker, a lamellar mesostructured material (BeIM-MIF) with a significantly increased periodicity of 8 nm results from the self-assembly of a highly crystalline 2D coordination polymer of [Zn(BeIM)OAc] interleaved with CTAB at regular intervals. The metal-organic layers are composed of stacks of nanosheets with a precisely defined number of layers, with each stack being separated by CTAB. Exfoliation of the layered composites under ultrasonication in organic solvents allows isolation of the nanosheet stacks to yield sheet and belt-like nanostructures with lateral dimensions of 10s to 100s of nm and a height which precisely matches that of the basal spacing of the mesostructure. Further, the flexible sheet-like nanostructures can roll up to form multi-walled coordination polymer nanotubes.

Most recently, Wu et al.[31] reported a successful co-templating strategy using CTAB and the amino acid L-histidine (His) as SDAs to produce hierarchically porous ZIF-8 in water under ambient conditions. (Figure 7a) His acts as a chelating agent for Zn(II) forming a stable interaction between the micelles and the metal ions using a similar $S^+A^-M^+$ (fig. 1c) assembly mechanism reported for the cooperative formation of mesoporous HKUST-1 from CTAB and citric acid.[20] The amino acid plays a key role in stabilization of the CTAB micelles and avoids the production of unwanted by-products by pre-chelating the Zn(II) ion, thus promoting the construction of phase pure ZIF-8 with enhanced crystallinity containing interconnected micro- and mesopores.

No typically hierarchical ZIFs were formed in the presence of either the CTAB or His separately (figure 7a); in addition to confirming the cooperative nature of the templating process, in both cases crystallinity of the water-synthesised ZIF-8 was improved. The mesopore distribution was centred at 22 nm and the high specific surface areas and pore volumes of hierarchically porous ZIFs led to highly efficient uptake capacities for the arsenate anion, a common inorganic water pollutant. Performance of the mesoporous ZIF-8 for arsenate adsorption was significantly better than commercial carbon and zeolites (fig 7b), where uptake was almost double that reported for standard microporous ZIF-8 prepared in water, arising directly from the templated porous structure.[31]

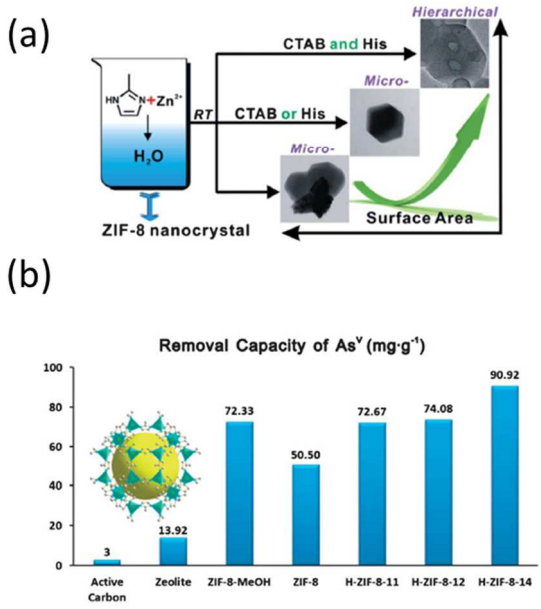

Figure 7. (a) Schematic representation of the formation of hierarchically porous ZIF-8 in the presence of CTAB and histidine as cooperative SDAs. (b) Comparison of the removal capacity of As^V by commercial active carbon, zeolite, normal ZIF-8 synthesized in water, ZIF-8 synthesized in methanol, and hierarchically structured ZIF-8 with different CTAB : His molar ratios: 1 : 1, 1 : 2, 1 : 4 (unadjusted pH value, initial concentration of As^V: 5.0 mg L^{-1}, dose (m V^{-1}) = 40 mg L^{-1}, t = 24 h, T = 25 _C, performed in triplicate). (Reprinted with permission from ref. 31. Copyright 2013 Royal Society of Chemistry)

3.2 Templating with anionic structure-directing agents

Anionic surfactants are used to a much lesser extent than their positively charged counterparts despite the potential for direct coordination bonds and hence increased interaction strength of the S^-M^+ type (fig 1b) between the SDA and the metal ion precursor. The S^-M^+ interaction has been clearly demonstrated by Kitagawa and co-workers, who effectively used amphiphilic dodecanoic acid (DDA, Fig S4) as a coordination modulator to control the size of HKUST-1 crystals from 20 nm to 2 μm in a microwave-assisted synthesis.[32] The DDA essentially binds to the Cu^{2+} ions to modulate the nucleation rate of the framework: small amounts of DDA favour fast nucleation and thus formation of smaller nanocrystals, which further aggregate into hierarchically porous phases with inter-particle mesoporosity.

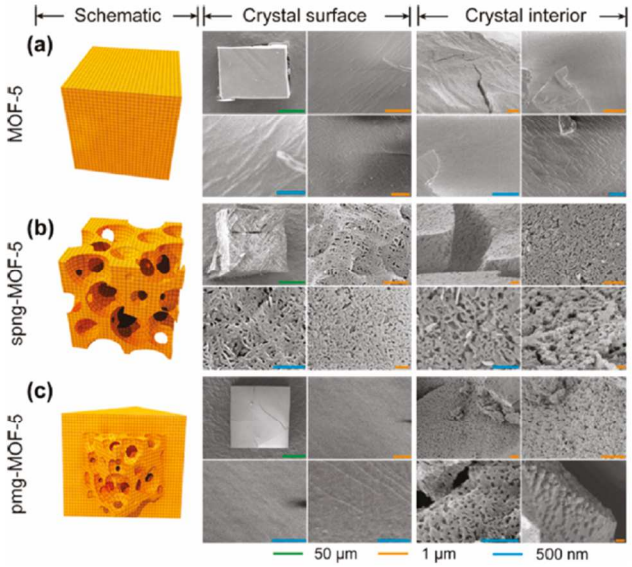

Figure 8. Pore structures of parent MOF-5 and its derivatives, spng-MOF-5 and pmg-MOF-5, formed in the presence of 4-(dodecyloxy)benzoic acid (DBA). SEM images of their crystal surface and interior of spng-MOF-5 and pmg-MOF-5 (scale bars, green 50 µm, orange 1 µm, blue 500 nm) clearly reveal the hierarchical nature of the porosity arising from space-filling by the DBA. (Reprinted with permission from ref. 15. Copyright 2011 American Chemical Society)

The anionic form of 4-(dodecyloxy)benzoic acid (DBA, fig S4) has been employed for the preparation of hierarchically porous MOF-5 [$Zn_4O(BDC)_3$ BDC = 1,4-benzenedicarboxylate] crystals, where sponge and pomegranate-like arrangements of meso- and macropores in the range of 10-100 nm were observed in spatially controlled locations within the MOF crystals.[15] (Figure 8) In the presence of equimolar amounts of DBA and the organic linker, the resulting MOF-5 crystals display macropores throughout giving rise to a sponge-like appearance (spng-MOF-5), but when the amount of DBA is reduced to 30 mol% the MOF-5 pomegrante-type structures (pmg-MOF-5) consisting of a spongeous interior enclosed by a thick crystalline outer shell of the pure microporous MOF-5. (Figure 8) It is clear that under these experimental conditions an ordered mesophase is not formed by the anionic DBA surfactant, although this clearly plays a dual role in the formation of hierarchically porous MOF-5: the hydrophilic carboxylate headgroup is used for binding to the Zn^{2+} ions required for framework formation while the long alkyl chain is used for space filling. Clearly the differing morphologies are strongly correlated to the availability of DBA during the crystal growth.

The CO_2 adsorption isotherms[15] of pmg-MOF-5 show a distinct hysteretic profile, and in spite of its lower surface area, the uptake capacity is 30% higher than standard microporous MOF-5. This behaviour is consistent with CO_2 uptake first through the microporous surface shell, followed by filling of the larger interior meso- and macropores under higher pressure followed by release through micropores as pressure is reduced. This behaviour is similar to that observed for MOF@MOF composites[33] composed of a large-pore MOF core encased by a smaller-pore MOF shell, where the former provides increased storage capacity for guest molecules that have been selectively adsorbed through the latter, strongly indicating that templating is a highly effective and facile strategy to prepare hierarchically porous MOFs with enhanced adsorption characteristics.

3.3 Templating with non-ionic block copolymers

In addition to the ionic surfactant SDAs outlined in sections 3.1 and 3.2, non-ionic templates including neutral surfactant molecules and block copolymers[34] have also been used to direct the formation of hierarchically porous MOFs. Block copolymers are composed of two or more macromolecular regions (or blocks) which have differing functionality or physical properties. When these regions differ in their hydrophilicity/hydrophobicity the block copolymers behave as typical amphiphiles and can self-assemble into wide-ranging structures such as spherical micelles, cylinders or rods, as well as forming cubic, hexagonal and lamellar type mesophases. This amphiphilic behaviour ensures they are increasingly popular and versatile SDAs for the templating of mesoporous materials with larger pores and narrow size distributions.[34] The block copolymers employed as SDAs are often of the Pluronic® type and are composed of blocks of ethylene oxide (EO) and propylene oxide (PO). A typical example is P123 – a triblock copolymer of composition ($EO_{20}PO_{70}EO_{20}$) where a hydrophobic poly-PO block is flanked either side by more hydrophilic poly-EO – that has previously been employed for the preparation of large-pore silica SBA-15.

The non-ionic triblock copolymer F127 ($EO_{97}PO_{69}EO_{97}$) has recently been employed as a supramolecular template for the synthesis of hierarchically porous HKUST-1, and $[Cu_2(HBTB)_2]$ (where H_3BTB = 1,3,5-tris[4-carboxyphenyl]benzene).[35] Pham et al prepared nanocrystals of HKUST-1 in an ethanolic reaction medium that displayed bimodal micro- and mesoporosity. Their dual strategy employed F127 to template mesopores within the MOF crystals in the presence of acetic acid (AA) to act as a coordination and (potential) deprotonation modulator. The AA enhances mesopore formation by slowing the crystallisation rate of the framework, permitting effective co-assembly with the triblock copolymer template by reducing framework growth and crystal size which prevents premature phase segregation. Higher crystallinity and more uniform wormhole-like mesostructures were obtained by increasing the AA/Cu^{2+} molar ratio, demonstrating its key role in the formation of both the micro- and mesopore structures within the MOF crystals.

For HKUST-1 prepared from an AA/Cu^{2+} molar ratio of 6:1, the non-aggregated 100-200 nm octahedral crystals display a narrow mesopore diameter of 4 nm which is comparable to that observed in SBA-16 silica templated by the same F127 SDA. HRTEM images indicate the octahedral mesocrystals are constructed from nanoscale crystallites, most likely by embedding along the hydrophilic EO blocks of the template chains to form the crystalline mesopore walls.

The combination of F127 and AA to control MOF crystal growth has also been reported by the same group for the preparation of nanocrystals of Fe-MIL-88B-NH_2 with tailored aspect ratios.[36] However, in this wholly aqueous synthesis no mesopore templating was observed, despite the 2-aminoterephthalic acid linker bearing two differing metal-binding functionalities which could potentially enhance interactions with the template.[23] This provides further evidence for the importance of the reaction solvent to successful templating of hierarchically porous MOFs.

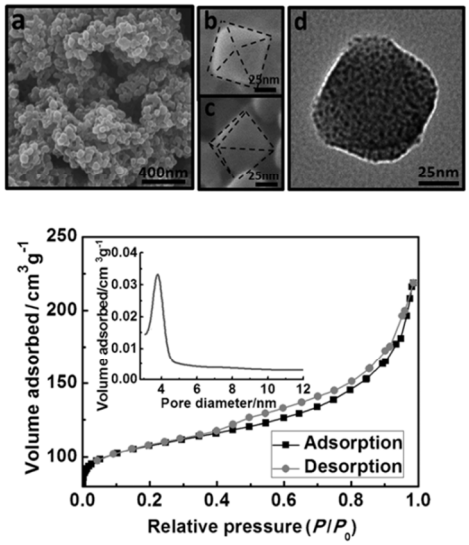

Figure 9. (top, a-d) SEM and TEM images of hierarchically porous HKUST-1 templated by PEG-300. (bottom) N_2 adsorption–desorption isotherms and mesopore size distribution (inset) of the nanocrystals shown above. (Reprinted with permission from ref. 37. Copyright 2014 Wiley-VCH)

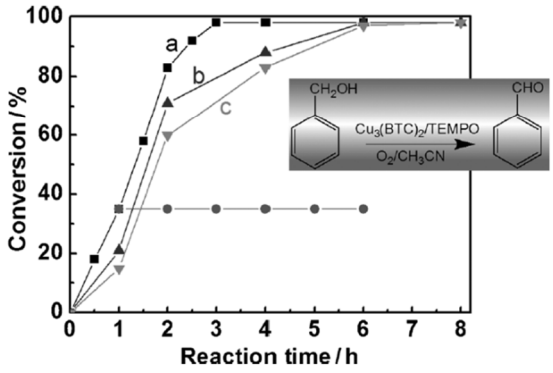

Figure 10. Time-conversion plots for the aerobic oxidation of benzyl alcohol to benzaldehyde catalyzed by HKUST-1 structures synthesized with PEG-300 (a), PEG-400 (b), and PEG-600 (c) (reaction conditions: temperature: 75 °C; benzyl alcohol 0.185 mmol, catalyst 30 mg, acetonitrile 1 mL, TEMPO 5 mg, oxygen atmosphere). The horizontal line shows the conversions upon removing the solid catalyst (synthesized in PEG-300) after 1 h and continued up to 6 h. (Reprinted with permission from ref. 37. Copyright 2014 Wiley-VCH)

Mesoporous HKUST-1 nanocrystals have also been prepared in the presence of poly(ethylene glycol) (PEG) and the triblock copolymer P104 ($EO_{27}PO_{61}EO_{27}$), where PEG rather than AA controls the crystallisation rate while P104 acts as the SDA to template mesopores within the crystals.[37] The PEG additive also becomes incorporated into the MOF pores through hydrogen bonding interactions of the S^0L^0 type (fig. 1d) where it acts as a strut to stabilise the mesopores against collapse after template and solvent removal. TEM images (fig 9, top) reveal the 60 nm octahedral MOF crystals are composed of ultrafine crystallites (2-3 nm) which form a disordered mesopore structure with a pore size of 3-4 nm, consistent with the pore size distribution obtained from N_2 adsorption isotherms. (Figure 9, bottom) Overall mesoMOF crystal size is tuneable by PEG molecular weight, where the more hydrophilic shorter chain analogues yield smaller crystals due to increased interaction with the ligands further suppressing framework growth.

The hierarchically porous HKUST-1 nanocrystals proved to be highly efficient heterogeneous catalysts for the oxidation of benzyl alcohol with selectivities for benzaldehyde > 98% and a near-quantitative conversion after 3 hrs.[37] (Figure 10) By comparison, commercial wholly microporous HKUST-1 only reached a conversion of 10% over the same period under identical conditions. The increased activity for the templated nanocrystals is attributed to the reduced particle size and mesopore structure providing efficient diffusion of substrates and products to the catalytically active sites by reduced path length and increased transport through larger pores.

Yuan and co-workers also exploited the supramolecular self-assembly of F127 to prepare a range of crystalline mesoMOFs based on pillared-layer metal disulphonate networks.[17] Well-defined hexagonal mesopores were prepared only in the presence of 18-crown-16 (1,10-diaza-18-crown-6), and in its absence only dense metal-sulphonate crystals arising from SDA exclusion due to increased reaction rate. The 18-crown-6 efficiently chelates the metal ions to control their release during the assembly and crystal growth process, facilitating the templating of stable mesopores. An assembly mechanism analogous to $(S^0H^+)A^-M^+$ (fig. 1f), where A^- corresponds to the sulphonate linker, is proposed based on the acidic nature of the synthesis mixture which was adjusted to pH 2.5-3. $[Cd(1,5\text{-NDS})(H_2O)_2]$ (1,5-NDS = 1,5-naphthalenedisulfonate) prepared in this way has a hexagonal arrangement of mesopores with a periodicity of 13-14 nm (figure 11) and is thermally stable to 300 °C.

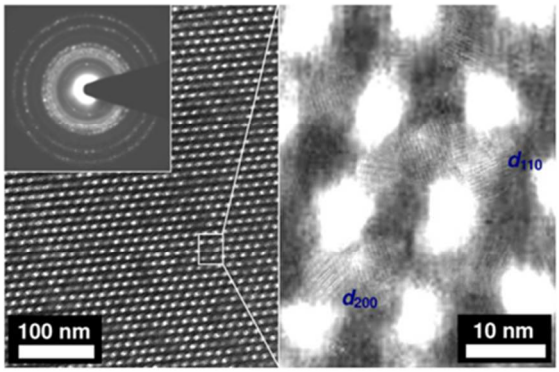

Figure 11. TEM images and electron diffraction pattern highlighting the periodic hexagonal arrangement of mesopores in $[Cd(1,5\text{-NDS})(H_2O)_2]$ templated by block copolymer F127 in the presence of 18-crown-16. (Reprinted with permission from ref. 17. Copyright 2012 American Chemical Society)

Kaliaguine and co-workers[38] have prepared hierarchically mesostructured MIL-53(Al) using P123 and F127 as SDAs under solvothermal conditions. In both cases the walls delineating the mesopores were composed of nanocrystals of microporous MIL-53(Al), and the presence of pores across both size regimes was confirmed by intermediate type I/IV N_2 adsorption isotherms. Interestingly, steps were observed in the hysteresis loop of the desorption branch corresponding to the removal of gas from two regular mesopore systems of different dimensions. These materials thus display trimodal porosity, and in addition to the inherent micropores of the MOF itself, the mesopore diameters were centred at 7.6 and 5.4 nm for the P123 and F127 templated samples respectively, with a further mesopore system at 4 nm in both phases arising specifically from the presence of EtOH in the synthesis. The 4 nm

mesopores also occur in MIL-53(Al) samples in the absence of the triblock copolymer SDAs, and suggest that certain solvent combinations could further enhance porosity.

Although the PO and EO blocks of Pluronic® type block copolymers appear effective as SDAs for the templating of mesoMOFs, their polyether functionalities are only weakly interacting with the metal ions and ligands that form the extended framework structures.[39] In an attempt to increase interactions with the SDA, Cao et al[40] used RAFT polymerisation strategies to prepare bespoke mesoscale block co-oligomers bearing the pyridine or carboxylate functionalities typically found in many framework-forming organic linkers. The block co-oligomers had the chemical composition $PSty_{14}$-*b*-$P4VP_{19}$ and $PSty_{14}$-*b*-PAA_{19} (PSty = polystyrene; P4VP = poly-4-vinylpyridine; PAA = polyacrylic acid), where a short hydrophobic polystyrene block is adjacent to a slightly longer hydrophilic one containing the desired metal-binding groups. $PSty_{14}$-*b*-$P4VP_{19}$ and $PSty_{14}$-*b*-PAA_{19} readily assemble into spherical micelles and dynamic light scattering revealed these to have diameters of 19 and 36 nm, respectively, which were used to directly template hierarchically porous analogues of the prototypical MOFs ZIF-8 and HKUST-1.[40]

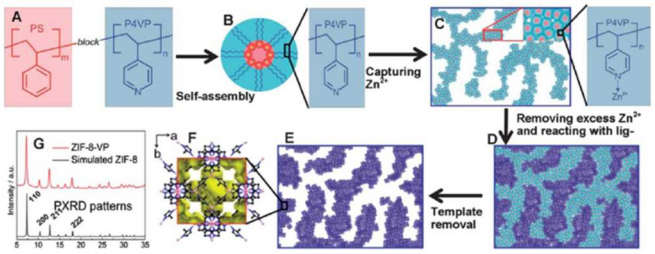

Figure 12. Synthesis mechanism for the formation of hierarchically porous ZIF-8 templated from block co-oligomer micelles. (Reprinted with permission from ref. 40. Copyright 2013 Royal Society of Chemistry)

After self-assembly of the block co-oligomer templates under appropriate conditions of pH, the metal-binding functionalities on the micelle exterior are cross-linked by the MOF precursor metal ions which bridge the micelles into a continuous 3D co-assembled network. (Figure 12a-c) This network provides preferential sites for MOF nucleation upon addition of the organic linking groups, where MOF nanocrystals intergrow along the contours of the co-assembled template. (Figure 12d) The final step involves removal of the SDAs by selective dissolution in organic solvents to leave hierarchically porous MOF materials that display branched fibrillar microstructured networks (figure 12e) of interconnected 40 nm crystallites reminiscent of the (micro)structure of silica aerogels. While the individual crystals do not contain templated mesopores, it is clear that the interconnected textural void channels form a bicontinuous architecture, and in all cases the templated materials show additional meso- and macroporous regions and higher total pore volumes than their single crystal analogues.

The use of non-Pluronic® block copolymer SDAs is well established for the preparation of high performance mesoporous materials with ultra-large pores and diverse pore symmetries not accessible using commercial EO-PO-EO type systems.[41] This is in part due to their ease of synthesis via facile living polymerisation methods and the greater degree of control over the functionality, constituent block size and molecular weight resulting in tailor-made templates for wide-ranging materials and properties. This seems a promising strategy toward mesoMOFs where tuneable coordination-based interactions with the template could be advantageous.

3.4 Templating with non-ionic surfactants

Hierarchically porous MOF nanospheres have been synthesised by Zhao et al using an ionic liquid (IL) and supercritical CO_2 ($scCO_2$) based emulsion system in the presence of the non-ionic surfactant N-ethyl perfluorooctylsulfonamide (N-EtFOSA; shown in fig 13, top) as both SDA and (emulsion) stabiliser.[42] Here the surfactant molecules self-assemble into cylindrical micelles with the fluorocarbon chain directed towards the micelle interior, where the $scCO_2$ exists at the core of the micelles. The IL forms the continuous phase between the micelles and is used to solubilise the metal ion and ligand components for MOF formation, which form a crystalline microporous framework punctuated by the micellar cavities. Consequently, MOFs with well-ordered mesopores and microporous structured walls were fabricated after removal of the IL, CO_2, and surfactant. The sizes of the micro- and mesopores determined by nitrogen adsorption isotherms were 0.7 and 3.0 nm respectively, with a mesopore wall thickness of 2.5 nm. The strong interaction between the fluorocarbon chains of N-EtFOSA and $scCO_2$ is vital to the formation of the mesopores, as materials prepared only in the IL have no mesoporous structure.

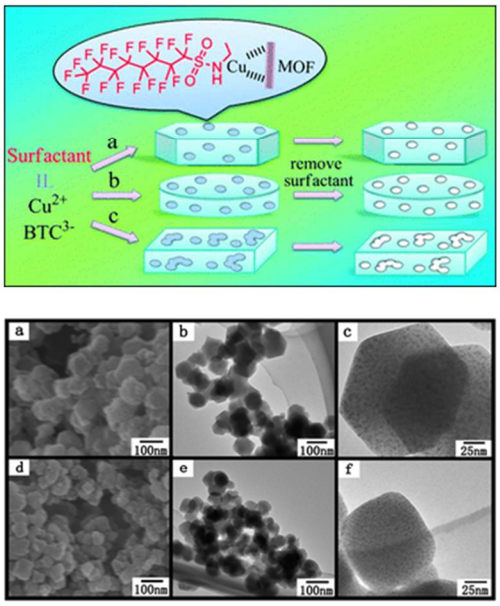

Figure 13. (top) Schematic illustration of the formation of mesoporous HKUST-1 nanoplates in surfactant–IL solutions at low (a), medium (b) and high (c) surfactant concentrations. (bottom) SEM and TEM images of the MOFs synthesized in 0.05 wt% (a–c) and 5 wt% (d–f) N-EtFOSA solutions highlighting the different crystal morphologies and the mesoporosity. (Reprinted with permission from ref. 43. Copyright 2012 Royal Society of Chemistry)

The same surfactant was employed by Peng et al.[43] to generate mesoporous HKUST-1 nanoplates from IL solutions, where plate morphology was strongly dependent on surfactant concentration. (Figure 13) SEM and TEM studies reveal that hexagonal, round and square-shaped plates are accessible at surfactant concentrations of 0.05, 2 and 5 wt%, respectively. In all cases the plate-like crystals displayed well-defined mesopores of 2.5 nm in diameter, and the ratio of meso-

/micropore surface area increases with increasing surfactant concentration. In all three systems studied, the surfactant concentration was below the critical micelle concentration of N-EtFOSA in the IL (10 wt%) implying that self-assembled micellar structures are not responsible for templating the mesoporosity. It is noted however, that in the absence of the surfactant no mesoporosity is observed.

It is proposed that the Cu^{2+} metal ions dissolved in the IL react with the deprotonated BTC^{3-} linkers to form nanosized framework building blocks, which are likely to be surface-stabilised by interaction with the N-EtFOSA surfactant molecules. These building blocks then co-assemble to form the mesostructured MOF particles. In this assembly process the surfactant plays a double role. Firstly, the surfactant molecules stabilising the nanosized building blocks form mesopores within the structure, and also acts as a directing agent that selectively adsorbs onto the crystallographic planes of the MOF to kinetically regulate the rate of framework extension and hence crystal growth to form the observed platelets.

3.5 Transformation of templated oxide mesostructures

It has recently been shown that metal oxides can be transformed into MOFs by direct reaction with the ligand component under appropriate synthetic conditions.[44] Typically the oxide acts as the metal source for the formation of a MOF seed layer that can readily undergo a secondary growth step for the preparation of high quality supported MOF membranes for gas and enantioselective separations. Currently there are significantly more ways to template or process oxides into mesoporous materials[45] or other architectures[46] than there are for MOFs. Hence, an alternative strategy to the direct templating methods reviewed here would be to template an oxide and then transform this into the desired MOF by reaction with a suitable ligand component.

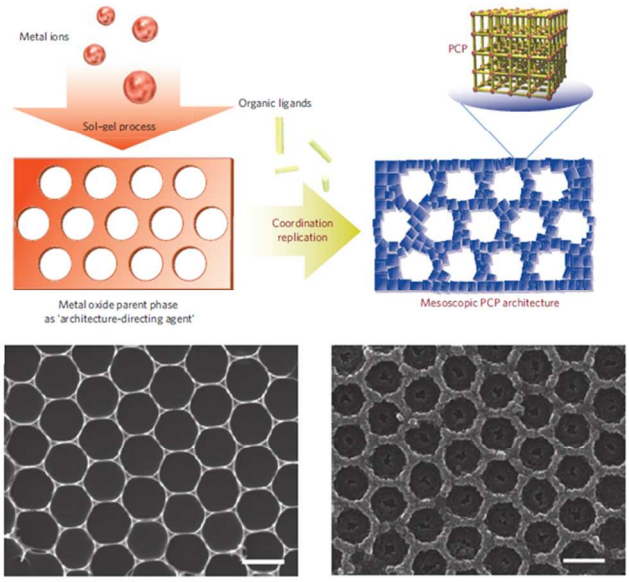

Figure 14. (top) Illustration of the transformation of a templated metal-oxide phase into a coordination framework replica by direct reaction with the ligand component. (bottom) SEM images (scale bars 1μm) of an alumina honeycomb network (left) and the resulting [Al(OH)(NDC)] MOF replica (right). (Adapted with permission from ref. 47. Copyright 2012 Nature Publishing Group)

Reboul et al[47] have elegantly demonstrated this concept by preparing a range of mesoscopic architectures of an aluminium dicarboxylate framework, [Al(OH)(NDC)] (where NDC = naphthalene dicarboxylate), where shaped alumina supports act simultaneously as a sacrificial metal source for MOF formation and an architecture-directing agent as shown in figure 14 (top). Two-dimensional honeycomb (figure 14, bottom) and 3-dimensional inverse opal structures of alumina were readily converted into [Al(OH)(NDC)] replicas by direct reaction with the ligand in water facilitated by microwave irradiation. Conversion to the MOF appears quantitative and no peaks for unreacted alumina are observed by diffraction measurements. This is further confirmed by microscopy studies following reaction, which reveal the alumina walls of the honeycomb and inverse opal architectures are replaced by intergrown 10-200 nm cubic crystals of the MOF. (figure 14, bottom) Clearly the MOF product inherits the shape of the alumina support, which strongly supports a coupled dissolution-reprecipitation mechanism of formation where the metastable alumina dissolves in the fluid at the solid/liquid interface, and immediately crystallizes as a new stable MOF phase at the same site as the dissolved precursor.

Randomly oriented alumina aerogels were also successfully converted into hierarchically porous MOF replicas with pores spanning the mesoporous or meso-/macroporous regimes depending on the pore structure of the template[47]. The aerogels of [Al(OH)(NDC)] contain hydrophobic micropores and were subsequently investigated for their ability to separate water and ethanol. Breakthrough experiments revealed a reduction in breakthrough time and inlet pressure when compared to the bulk powder and increased selectivity when compared to the parent macroscopic alumina aerogel. This strongly indicates that processing of MOFs into hierarchically porous structures is an excellent strategy to enhance their properties in applications such as separation and catalysis.

4. Conclusions and outlook

There are clear advantages to increasing the pore size of MOFs into the mesoporous regime, where the larger pores can permit accelerated adsorption kinetics due to improved mass transport, with enhanced accessibility and overall storage capacity for large molecules. As this review shows however, reliable templating of hierarchically porous MOFs using supramolecular aggregates of surfactants or other amphiphilic species remains a current challenge that is only now beginning to be addressed. Several factors need to be carefully balanced during synthesis, particularly relating to the co-assembly of the template and the MOF building blocks to prevent premature phase segregation, which can in part be controlled through modulation of reaction kinetics. Careful systematic studies such as those carried out over the last three decades on siliceous materials will surely aid our understanding of the complex assembly processes involved for these hybrid frameworks, leading to new classes of hierarchically porous functional materials with controlled crystal size and morphology.

Mesoporous MOFs can provide an alternative to the hybrid periodic mesoporous organosilicas[48] that incorporate organic groups into the silica mesopore walls. This is achieved by using appropriate organosilane precursors, which are often difficult to make and limits these to relatively simple organic functionality. With MOFs however, both the (functional) organic and metal components are integral parts of the mesopore walls, so this also removes the need for the porosity reducing post-synthetic grafting strategies often employed to endow mesoporous silica with additional levels of functionality.

MOFs containing large mesoporous cages have previously excelled in applications typical for porous materials[7,8] (gas storage and separation, catalysis, drug delivery, separation, sensing) and this utility is expected to be further enhanced with hierarchically porous structures. The supramolecular templating of hierarchically porous MOFs however is still in its infancy, and as yet there are no demonstrable applications of these materials under real or simulated operating conditions of catalytic or separation processes. One recent exception that hints at their potential is hierarchically micro- and macroporous HKUST-1, where macroporous channels etched into pre-formed MOF crystals significantly enhances the liquid phase separation of aromatic molecules when used as a stationary phase in HPLC.[49]

Mesoporosity also plays a significant role in catalysis, especially in challenging processes where bulky molecules such as those obtained from biomass, or highly unreactive species such as CO_2, can be transformed into high value products.[6] Furthermore, mesoporous materials also play a significant role as electrodes in fuel and solar cells and in thermoelectric devices: technologies which are all within the capabilities of MOFs. The ability to fine tune the pore chemistry of MOFs in a highly controlled manner will allow the internal surfaces of the resulting large pore mesoMOFs to be optimised for interaction with biological molecules for chemoenzymatic tandem catalysis or for proteomics and sequencing.[50] The potential of such materials and their composites is great, and the challenge is now set to obtain highly ordered and stable mesoporosity into MOFs that is on a par with that observed for silicas. While this will certainly constitute an important step to widening and enhancing MOF applications, the development of strategies for scale-up should not be forgotten. Some prototypical MOFs have already been prepared on a large scale, so modifying these preparations to ensure their compatibility with supramolecular templating as described in this article would be an excellent starting point to realise this goal.

Acknowledgements

We gratefully acknowledge the European Research Council for funding (ERC-StG2010-BIOMOF-258613)

Notes and references

[a] School Of Chemistry, University of Southampton, Highfield, Southampton SO17 1BJ, U. K. E-mail: D.Bradshaw@soton.ac.uk; Tel: +44(0)2380599076

1. S. Kitagawa, R. Kitaura and S. Noro, *Angew. Chem., Int. Ed*., 2004, **43**, 2334.
2. G. Fe´rey, *Chem. Soc. Rev*., 2008, **37**, 191.
3. M. Eddaoudi, J. Kim, N. Rosi, D. Vodak, J. Wachter, M. O'Keeffe and O. M. Yaghi, *Science*, 2002, **295**, 469.
4. MOF special issue, *Chem. Soc. Rev*. 2009, **38**, 1201 (19 articles)
5. Z. Wu and D. Zhao, *Chem. Commun*. 2011, **47**, 3332.
6. N. Linares, A. M. Silvestre-Albero, E. Serrano, J. Silvestre-Albero and J. Garcia-Martinez, *Chem. Soc. Rev*. 2014, DOI 10.1039/c3cs60435g.
7. Q.-R. Fang, T. A. Makal, M. D. Young and H.-C. Zhou, *Comments on Inorg Chem* 2010, **31**, 165.
8. W. Xuan, C. Zhu, Y. Liu and Y. Cui, *Chem. Soc. Rev*. 2012, **41**, 1677..
9. H. Deng et al, *Science* 2012, **336**, 1018.
10. X. Roy and M. J. MacLachlan, *Chem. Eur. J*. 2009, **15**, 6552.
11. C. T. Kresge, M. E. Leonowicz, W. J. Roth. J. C. Vartuli and J. S. Beck, *Nature* 1992, **359**, 710.
12. W. Li, D. Zhao, *Chem. Commun*. 2013, **49**, 943.
13. Y. Wan, D. Zhao, *Chem. Rev*. 2007, **107**, 2821.
14. L.-G. Qiu, T. Xu, Z.-Q. Li, W. Wang, Y. Wu, X. Jiang, X.-Y Tian and L.-D. Zhang, *Angew. Chem., Int. Ed*., 2008, **47**, 9487
15. K. M. Choi, H. J. Jeon, J. K. Kang and O. M. Yaghi, *J. Am. Chem. Soc*. 2011, **133**, 11920.
16. L.-B. Sun, J.-R. Li, J. Park and H.-C. Zhou, *J. Am. Chem. Soc*. 2012, **134**, 126.
17. T.-Y. Ma, H. Li, Q.-F. Deng, L. Liu, T.-Z. Ren and Z.-Y. Yuan, *Chem. Mater*. 2012, **24**, 2253.
18. E. A. Flugel, A. Ranft, F. Haase and B. V, Lotsch, *J. Mater. Chem*. 2012, **22**, 10119.
19. I. I. Slowing, B. G. Trewyn, S. Giri and V. S.-Y. Lin, *Adv. Funct. Mater*. 2007, **17**, 1225.
20. S. S.-Y. Chui, S. M.-F. Lo, J. P. H. Charmant, A. G. Orpen and I. D. Williams, *Science*, 1999, **283**, 1148.
21. X.-X. Huang, L.-G. Qiu, W. Zhang, Y.-P. Yuan, X. Jiang, A.-J. Xie, Y.-H. Shen and J.-F. Zhu, *CrystEngComm* 2012, **14**, 1613.
22. L. H. Wee, C. Wiktor, S. Turner, W. Vanderlinden, N. Janssens, S. R. Bajpe, K. Houthoofd, G. Van Tendeloo, S. De Feyter, C. E. A. Kirschhock and J. A. Martens *J. Am. Chem. Soc*. 2012, **134**, 10911.
23. Y. Li, D. Zhang, Y.-N. Guo, B. Guan, D. Tang, Y. Liu and Q. Huo, *Chem. Commun.*, 2011, **47**, 7809.
24. Y.-N. Guo, Y. Li, B. Zhi, D. Zhang, Y. Liu and Q. Huo, *RSC Advances*, 2012, **2**, 5424.
25. Y. Y. Pan, D. Heryadi, F. Zhou, L. Zhao, G. Lestari, H. Su and Z. Lai, *CrystEngComm* 2011, **13**, 6937.
26. K. S. Park, Z. Ni, A. P. Cote, J. Y. Choi, R. Huang, F. J. Uribe-Romo, H. K. Chae, M. O'Keeffe and O. M. Yaghi, *Proc. Natl. Acad. Sci. U. S. A*., 2006, **103**, 10186.
27. R. Banerjee, A. Phan, B. Wang, C. Knobler, H. Furukawa, M. O'Keeffe and O. M. Yaghi, *Science* 2008, **319**, 939.
28. H. Bux, F. Liang, Y. Li, J. Cravillon, M. Wiebcke and J. Caro, *J. Am. Chem. Soc*. 2009, **131**, 16000.
29. S. C. Junggeburth, K. Schwinghammer, K. S. Virdi, C. Scheu and B. V. Lotsch, *Chem. Euro. J.*, 2012, **18**, 2143.
30. S. C. Junggeburth, L. Diehl, S. Werner, V. Duppel, W. Sigle and B. V. Lotsch, *J. Am. Chem. Soc*., 2013, **135**, 6157.
31. Y.-N. Wu, M. Zhou, B. Zhang, B. Wu, J. Li, J. Qiao, X. Guan and F. Li, *Nanoscale*, 2014, **6**, 1105.
32. S. Diring, S. Furukawa, Y. Takashima, T. Tsuruoka and S. Kitagawa, *Chem. Mater.*, 2010, **22**, 4531.
33. K. Hirai, S. Furukawa, M. Kondo, H. Uehara, O. Sakata and S. Kitagawa, *Angew. Chem., Int. Ed*., 2011, **50**, 8057.
34. Y. Wan, Y. Shi and D. Zhao, *Chem. Commun*. 2007, 897.
35. P. Minh-Hao, V. Gia-Thanh, F.-G. Fontaine and D. Trong-On, *Crys. Grow. & Des.*, 2012, **12**, 1008.
36. P. Minh-Hao, V. Gia-Thanh, V. Anh-Tuan and D. Trong-On, *Langmuir*, 2011, **27**, 15261.
37. Z. Xue, J. Zhang, L. Peng, B. Han, T. Mu, J. Li and G. Yang, *ChemPhysChem*, 2014, **15**, 85.
38. X.-D. Do, H. Vinh-Thang and S. Kaliaguine, *Micro. Meso. Mater.*, 2011, **141**, 135.

39. J. Yao, M. He, K. Wang, R. Chen, Z. Zhong and H. Wang, *CrystEngComm*, 2013, **15**, 3601.
40. S. Cao, G. Gody, W. Zhao, S. Perrier, X. Peng, C. Ducati, D. Zhao and A. K. Cheetham, *Chem. Sci.*, 2013, **4**, 3573.
41. Y. Deng, J. Wei, Z. Sun and D. Zhao, *Chem. Soc. Rev.*, 2013, **42**, 4054.
42. Y. Zhao, J. Zhang, B. Han, J. Song, J. Li and Q. Wang, *Angew. Chem. Int. Ed.*, 2011, **50**, 636.
43. L. Peng, J. Zhang, J. Li, B. Han, Z. Xue and G. Yang, *Chem. Commun.*, 2012, **48**, 8688.
44. Y. Hu, X. Dong, J. Nan, W. Jin, X. Ren, N. Xu and Y. M. Lee, *Chem. Commun*., 2011, 737.
45. D. Gu, F. Schuth, *Chem. Soc. Rev*. 2014, **43**, 313
46. L. Qi, *Coord. Chem. Rev*. 2010, **254**, 1054.
47. J. Reboul, S. Furukawa, N. Horike, M. Tsotsalas, K. Hirai, H. Uehara, M. Kondo, N. Louvain, O. Sakata and S. Kitagawa, *Nat. Mater.*, 2012, **11**, 717.
48. F. Hoffmann, M. Cornelius, J. Morell and M. Froba, *Angew. Chem. Int. Ed*. 2006, **45**, 3216.
49. A. Ahmed, N. Hodgson, M. Barrow, R. Clowes, C. Robertson, A. Steiner, P. McKeown, D. Bradshaw, P. Myers and H. Zhang, *J. Mater. Chem. A*, 2014, DOI: 10.1039/C4TA00138A.
50. F. Li, B. Dever, H. Zhang, X.-F. Li and X. C. Li, *Angew. Chem. Int. Ed.*, 2012, **51**, 3518.

Key learning points:

1. The importance of hierarchically porous materials and the particular need to increase the pore size of MOFs.
2. How supramolecular templating strategies work and can be applied to MOFs.
3. Understand the factors that need to be balanced for successful templating of mesoporous MOFs.
4. Examples of successful templating and how these have enhanced the properties of MOFs in adsorption processes and catalysis.
5. Alternative strategies that are available for mesoMOFs, such as the direct conversion of templated oxide supports.

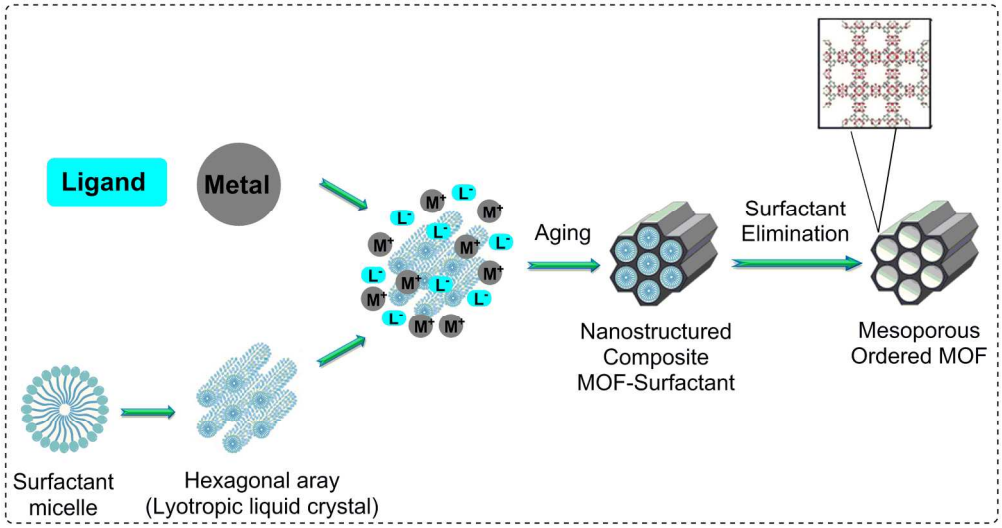

190x100mm (300 x 300 DPI)

Darren Bradshaw completed a PhD in Bioinorganic coordination chemistry under the supervision of Prof David E. Fenton at the University of Sheffield in 2001. Following this he moved to the University of Liverpool as a postdoctoral research associate working on metal-organic frameworks (MOFs) in the group of Prof Matt Rosseinsky FRS, and in 2005 took up a 5 year tenure track RCUK Academic Fellowship in materials discovery. He was appointed lecturer in inorganic chemistry at Liverpool in 2010, and was awarded a prestigious ERC starting grant the same year. In summer 2012 he took up a readership in the School of Chemistry at the University of Southampton. His research currently focuses on the growth and processing of MOFs into application-specific configurations.

Samir El Hankari was born in Morocco in 1982. He received his DESA (master) degree at the University of Mohammed V-Agdal Rabat in 2007, and his PhD in 2012 from the University of Montpellier 2 and Mohammed V-Agdal Rabat under the supervision of Dr Peter Hesemann and Professor Ahmed Bouhaouss. Currently he is a postdoctoral research associate with Dr Darren Bradshaw in the School of Chemistry at the University of Southampton. His research interests involve templating and processing of mesoporous MOFs and MOF-oxide composite materials and evaluating their practical application in catalysis and as chromatography stationary phases

Lucia Lupica Spagnolo received her MSc in Chemistry from the University of Parma, Italy, in 2011. She is currently a PhD student in the group of Dr Darren Bradshaw in the School of Chemistry at the University of Southampton. Her research focuses on the synthesis of mesoporous Metal Organic Frameworks with a surfactant templating approach.

Graphical abstract text:

This tutorial review summarises recent advances in the soft templating of metal-organic frameworks with hierarchical porosity across the micro- and mesoporous regimes.

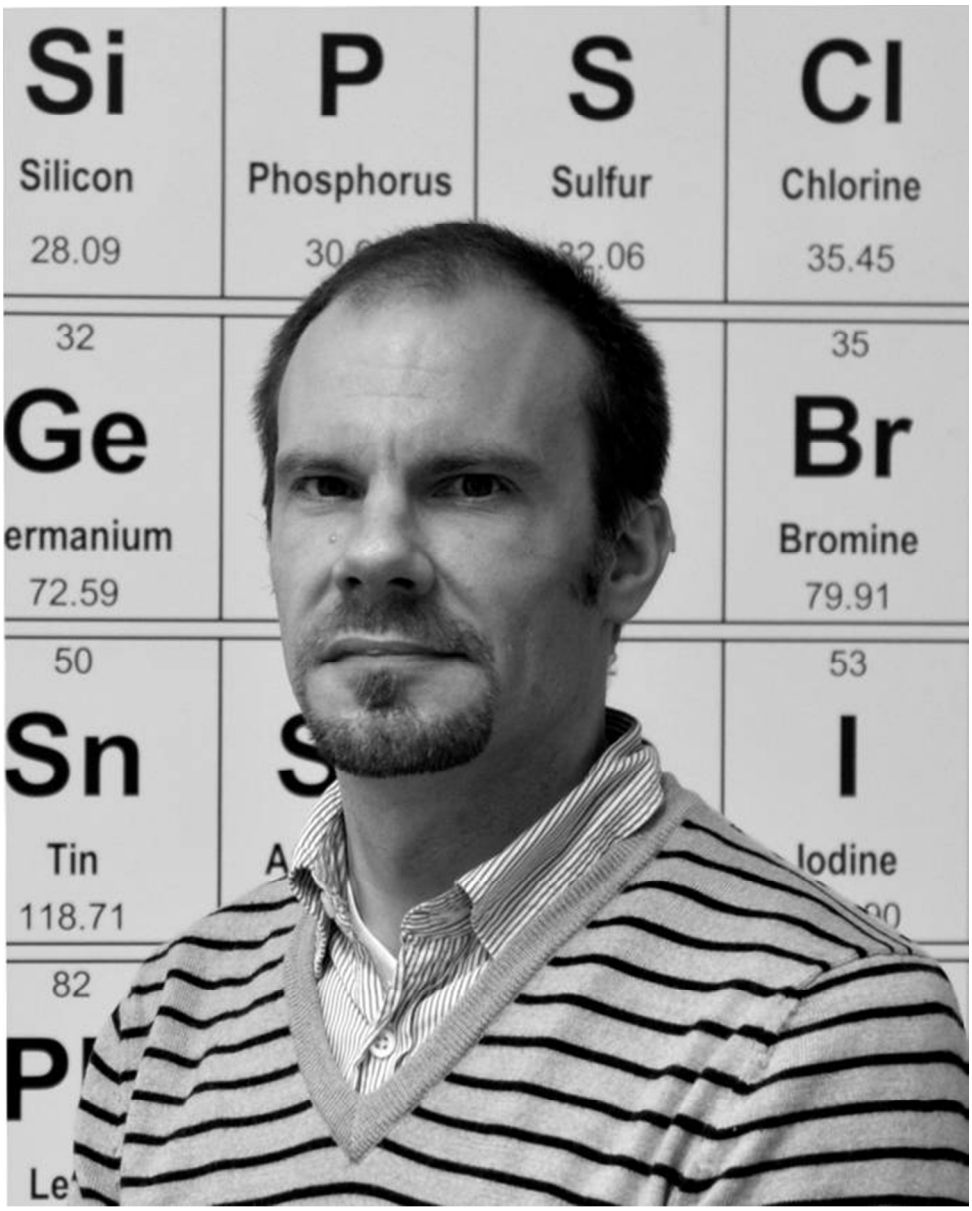

184x229mm (96 x 96 DPI)

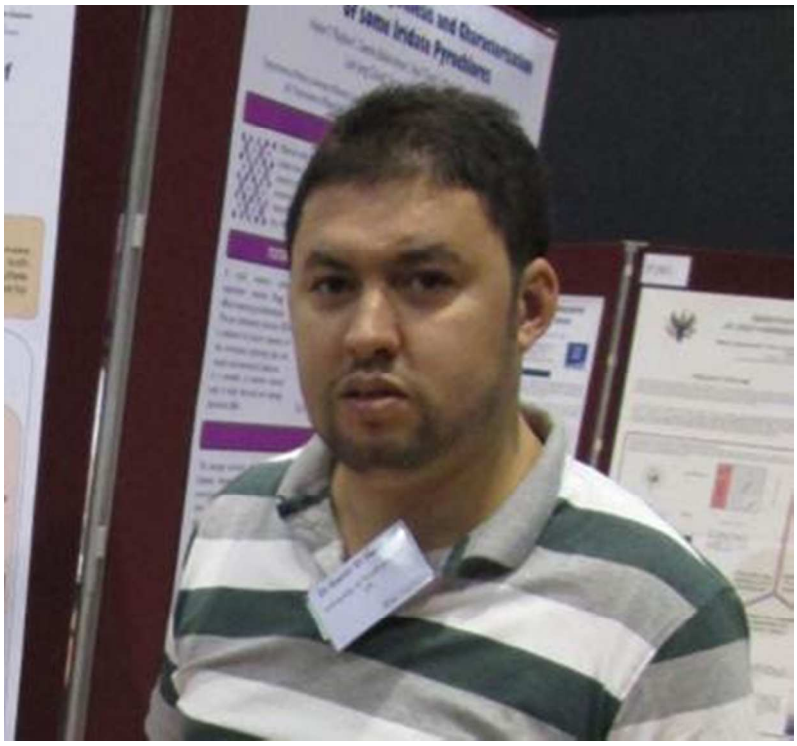

70x66mm (141 x 141 DPI)

63x65mm (96 x 96 DPI)